Journal of Cellular Physiology

Amyloid-β-Induced Reactive Oxygen Species Production and Priming Are Differentially Regulated by Ion Channels in Microglia

TOM SCHILLING AND CLAUDIA EDER*

Division of Biomedical Sciences, St. George's University of London, London, UK

Production of reactive oxygen species (ROS) by microglial cells and subsequent oxidative stress are strongly implicated in the pathogenesis of Alzheimer's disease. Although it is recognized that amyloid-β (Aβ) plays a major role in inducing and regulating microglial ROS production in Alzheimer's disease, to date little is known about cellular mechanisms underlying Aβ-stimulated ROS production. Here, we identified ion channels involved in Aβ-induced microglial ROS production and in Aβ-induced microglial priming. Acute stimulation of microglial cells with either fibrillar $A\beta_{1-42}$ ($fA\beta_{1-42}$) or soluble $A\beta_{1-42}$ ($sA\beta_{1-42}$) caused significant increases in microglial ROS production, which were abolished by inhibition of TRPV1 cation channels with 5-iodo-resiniferatoxin (I-RTX), but were unaffected by inhibition of K^+ channels with charybdotoxin (CTX). Furthermore, pretreatment with either $fA\beta_{1-42}$ or $sA\beta_{1-42}$ induced microglial priming, that is, increased ROS production upon secondary stimulation with the phorbol ester PMA. Microglial priming induced by $fA\beta_{1-42}$ or $sA\beta_{1-42}$ remained unaffected by TRPV1 channel inhibition with I-RTX. However, $sA\beta_{1-42}$-induced priming was inhibited by CTX and margatoxin, but not by TRAM-34 or paxilline, indicating a role of Kv1.3 voltage-gated K^+ channels, but not of Ca^{2+}-activated K^+ channels, in the priming process. In summary, our data suggest that in microglia Aβ-induced ROS production and priming are differentially regulated by ion channels, and that TRPV1 cation channels and Kv1.3 K^+ channels may provide potential therapeutic targets to reduce microglia-induced oxidative stress in Alzheimer's disease.

J. Cell. Physiol. 226: 3295–3302, 2011.

Accumulation of amyloid-β (Aβ) in the brain is a pathological hallmark of Alzheimer's disease and promotes the progression of this disease (Rodrigue et al., 2009; Querfurth and LaFerla, 2010). In Alzheimer's disease, Aβ is one of the major factors causing microglial activation (Schlachetzki and Hüll, 2009; Mandrekar-Colucci and Landreth, 2010), while reactive oxygen species (ROS) produced by activated microglial cells play a pivotal role in the pathogenesis of Alzheimer's disease. Extracellular ROS lead to oxidative stress and subsequent neuronal damage, while intracellular ROS act as signaling molecules enhancing the production of substances, which are known to promote neuro-inflammatory processes and to damage surrounding healthy neurons (Block, 2008). Thus, due to the detrimental effects of ROS produced by activated microglial cells in Alzheimer's disease, it is of particular interest to understand mechanisms underlying Aβ-induced microglial ROS production.

Microglial ROS production can be affected by Aβ via two distinct mechanisms, namely Aβ can (i) directly stimulate NADPH oxidase-mediated ROS production by microglial cells (El Khoury et al., 1996; McDonald et al., 1997; Bianca et al., 1999; Milton et al., 2008) and (ii) prime microglia, that is, prolonged/chronical exposure to Aβ results in the generation of microglial cells that are characterized by enhanced NADPH oxidase-mediated ROS production upon secondary stimulation (van Muiswink et al., 1996; Klegeris and McGeer, 1997; Colton et al., 2000). Mechanisms underlying Aβ-induced ROS production and priming are not fully understood.

Although growing evidence suggests that ion channels provide promising therapeutic targets in neurodegenerative and neuroinflammatory diseases (Judge et al., 2006; Rangaraju et al., 2009; Eder, 2010), to date little is known about the role of ion channels in Aβ-induced ROS production and priming. In this study, we aimed to identify microglial ion channels involved in these processes with the view of identifying potential novel therapeutic targets for the treatment of Alzheimer's disease.

Materials and Methods

Chemicals

The following agents were used in this study: $A\beta_{1-42}$ (Bachem AG, Weil am Rhein, Germany), $A\beta_{42-1}$ (Bachem AG), charybdotoxin (CTX; Latoxan, Valence, France), 5-iodo-resiniferatoxin (I-RTX; Tocris, Bristol, UK), margatoxin (MTX; Latoxan), paxilline, phorbol 12-myristate 13-acetate (PMA), 1-[(2-chlorophenyl)diphenylmethyl]-1H-pyrazole (TRAM-34). If not stated otherwise drugs were obtained from Sigma, Poole, UK. The following stock solutions were prepared in FCS-free DMEM: 500 μM $A\beta_{1-42}$, 500 μM $A\beta_{42-1}$, 20 μM CTX, 50 μM MTX, and the following stock solutions were prepared in DMSO: 2 mM I-RTX, 10 mM paxilline, 1 mM PMA, and 10 mM TRAM-34. To obtain fibrillar $A\beta_{1-42}$ ($fA\beta_{1-42}$) or fibrillar

Abbreviations: Aβ, amyloid-β; CTX, charybdotoxin; I-RTX, 5-iodo-resiniferatoxin; MTX, margatoxin; PMA, phorbol 12-myristate 13-acetate; TRAM-34, 1-[(2-chlorophenyl)diphenylmethyl]-1H-pyrazole

Contract grant sponsor: St. George's, University of London (start-up grant).
Contract grant sponsor: Wellcome Trust (Value in People Award).

*Correspondence to: Claudia Eder, Division of Biomedical Sciences, St. George's University of London, Cranmer Terrace, London SW17 0RE, UK. E-mail: ceder@sgul.ac.uk

Received 25 November 2010; Accepted 31 January 2011

Published online in Wiley Online Library (wileyonlinelibrary.com), 14 February 2011.
DOI: 10.1002/jcp.22675

$A\beta_{42-1}$ ($fA\beta_{42-1}$), 500 μM soluble $A\beta_{1-42}$ ($sA\beta_{1-42}$) or 500 μM soluble $A\beta_{42-1}$ ($sA\beta_{42-1}$), respectively, were incubated at 37°C for 1 day under sterile conditions as described previously (Jan et al., 2010).

Cells

All experiments were performed on BV-2 microglial cells, which resemble primary cultured microglia and microglia in brain tissue in their ion channel expression pattern as well as in their capability to produce ROS and to respond to Aβ (Blasi et al., 1990; Milton et al., 2008; Eder, 2010). BV-2 microglial cells were cultured permanently in DMEM supplemented with 10% FCS and 2 mM L-glutamine as described previously (Stock et al., 2006). Cells were split twice a week, and were plated on glass coverslips at a density of 1×10^5/ml for subsequent experiments.

During priming with Aβ in the absence or presence of ion channel inhibitors, cells were maintained for 24 h in FCS-containing DMEM culture medium. After the priming period, cells were washed twice with FCS-free DMEM and were subsequently stimulated with PMA in FCS-free DMEM for 1 h in the absence of Aβ and ion channel inhibitors.

Detection of reactive oxygen species

ROS generation was revealed by the ROS-sensitive dye DCFDA as described previously (Schilling and Eder, 2009). Microglial cells were incubated with 10 μM CM-H_2DCFDA for 1 h at 37°C in the cell culture incubator in FCS-free DMEM in the absence or presence of Aβ, PMA, and/or ion channel inhibitors as indicated. After stimulation, cells were washed and fluorescence intensity of cells was analyzed using an inverted microscope IX51 (Olympus, Hamburg, Germany) and the image processing software cell^D (Olympus, Southend-on-Sea, Essex, UK). For ROS measurements, the fluorescence imaging system consisted of a mercury lamp, a CCD camera (F-View II, Olympus, UK), an excitation filter of 480 ± 10 nm wavelength, a dichroic mirror of 505 nm wavelength and a barrier filter of 530 ± 20 nm wavelength (all from Olympus, Germany). Images of at least four different visual fields for at least three independent experiments per condition were collected and analyzed. Fluorescence intensities of all cells were corrected for background fluorescence.

Statistics

All data are presented as mean values ± standard error of the mean (SEM) and numbers of analyzed cells are indicated. The statistical significance of differences between experimental groups was evaluated by one-way ANOVA using the SPSS program. Tukey's test was used for post hoc comparison after confirming homogeneity of variances with Levene's test. Data were considered to be statistically significant with $P < 0.05$.

Results

Ion channels regulating microglial ROS production induced by acute stimulation with amyloid-β

Aβ can affect microglial behavior both in its fibrillar as well as in its soluble form. Figure 1 demonstrates acute effects of fibrillar amyloid-β (fAβ) and of soluble amyloid-β (sAβ) on microglial ROS production. Stimulation of microglia with either $fA\beta_{1-42}$ or $sA\beta_{1-42}$ significantly ($P < 0.001$ in both cases) increased microglial ROS production. Following stimulation of microglia with 5 μM $fA\beta_{1-42}$ for 4 h, mean DCFDA fluorescence intensity was increased to 164.2 ± 4.6% (n = 542), whereas the inactive form $fA\beta_{42-1}$ had no effect ($P = 0.853$) on microglial ROS production (Fig. 1A). Effects of $sA\beta_{1-42}$ on microglial ROS production occurred faster and were more pronounced than those of $fA\beta_{1-42}$. Following exposure of microglial cells to 5 μM $sA\beta_{1-42}$ for 1 h, microglial ROS production was increased to 400.4 ± 12.3% (n = 579; Fig. 1B). Under identical stimulation conditions, the inactive form $sA\beta_{42-1}$ did not induce significant ($P = 0.995$) increases in microglial ROS production (Fig. 1B). Example images in Fig. 1C demonstrate the effects of sAβ on microglial ROS generation as determined by changes in DCFDA fluorescence intensity.

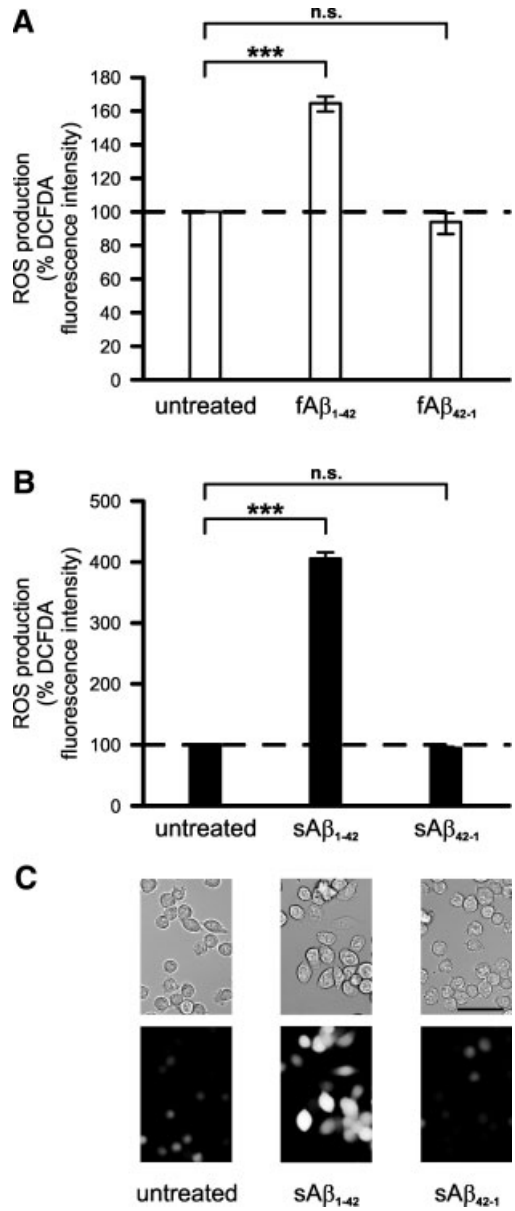

Fig. 1. Production of ROS by $fA\beta_{1-42}$- and $sA\beta_{1-42}$-stimulated microglial cells. Microglial ROS production was determined by DCFDA fluorescence imaging. A: Mean fluorescence intensities of DCFDA-loaded microglial cells kept untreated (n = 627), or stimulated with either 5 μM $fA\beta_{1-42}$ (n = 542) or 5 μM $fA\beta_{42-1}$ (n = 261) for 4 h. B: Mean fluorescence intensities of DCFDA-loaded cells kept untreated (n = 760) or stimulated with either 5 μM $sA\beta_{1-42}$ (n = 579) or 5 μM $sA\beta_{42-1}$ (n = 510) for 1 h. A,B: Fluorescence intensities of all cells were determined and normalized to the mean fluorescence intensities determined for untreated control cells. C: Brightfield images (upper row) and fluorescence images (lower row) of DCFDA-loaded microglial cells kept untreated or stimulated with either 5 μM $sA\beta_{1-42}$ or 5 μM $sA\beta_{42-1}$. Scale bar, 50 μm. ***$P < 0.001$; n.s., not significant.

Next we aimed to identify ion channels regulating $fA\beta_{1-42}$ and $sA\beta_{1-42}$-induced microglial ROS production. In our study we focused on TRPV1 cation channels as well as on voltage-gated and Ca^{2+}-activated K^+ channels, because these channels are expressed by microglia both in vitro and in vivo (Eder, 2010), and specific inhibitors are available for each of those ion channel types. As demonstrated in Fig. 2A, inhibition of TRPV1 channels with 100 nM I-RTX abolished ROS production by $fA\beta_{1-42}$-stimulated microglia ($P < 0.001$). Similar to the inhibitory effects of I-RTX on $fA\beta_{1-42}$-stimulated microglia, $sA\beta_{1-42}$-induced microglial ROS production was abolished upon inhibition of TRPV1 channels with 100 nM I-RTX ($P < 0.001$; Fig. 2B). Under control conditions without Aβ stimulation, I-RTX inhibited slightly, but not significantly ($P = 0.676$ in Fig. 2A, $P = 0.238$ in Fig. 2B) microglial ROS production.

To test whether K^+ channel activity is additionally required for $fA\beta_{1-42}$- and/or $sA\beta_{1-42}$-induced microglial ROS production, effects of charybdotoxin (CTX), which blocks voltage-gated as well as Ca^{2+}-activated K^+ channels in microglia (Eder, 1998, 2010), were investigated. As shown in Fig. 2C, $fA\beta_{1-42}$-induced microglial ROS production was not inhibited by 1 μM CTX ($P = 0.988$). Similarly, 1 μM CTX did not significantly affect ROS production by $sA\beta_{1-42}$-stimulated microglial cells ($P = 0.925$; Fig. 2D). Mean DCFDA fluorescence intensities of microglia stimulated with either $fA\beta_{1-42}$ or $sA\beta_{1-42}$ in the presence of CTX were 99.0 ± 1.9% (n = 379) and 99.1 ± 3.4% (n = 447), respectively, when compared with the corresponding mean DCFDA fluorescence intensities of $fA\beta_{1-42}$- and $sA\beta_{1-42}$-treated microglia kept in the absence of CTX.

In summary, these data indicate that TRPV1 cation channels, but not voltage-gated or Ca^{2+}-activated K^+ channels, regulate

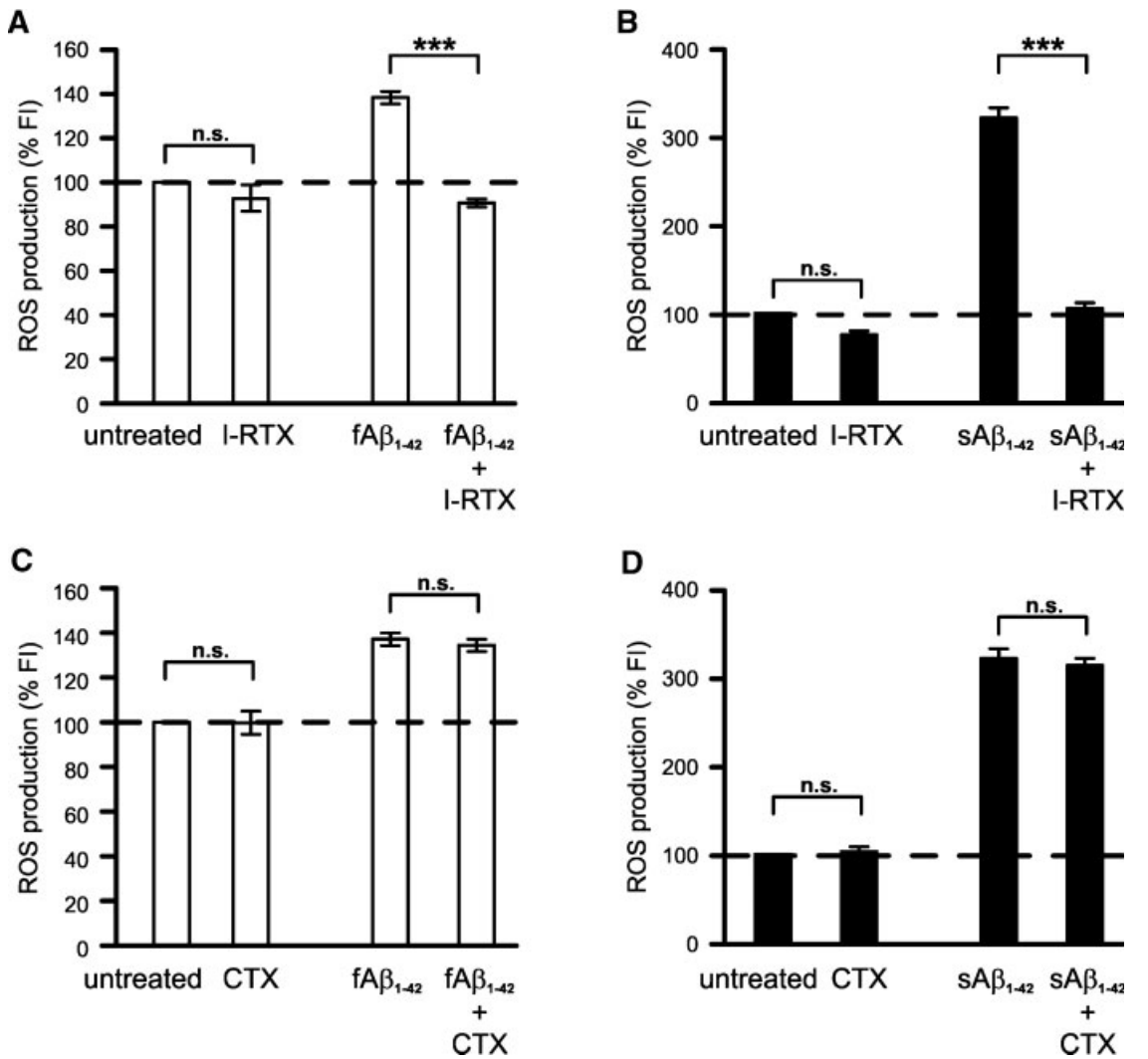

Fig. 2. Importance of ion channels for $A\beta_{1-42}$-induced ROS production. A: Inhibitory effects of TRPV1 channel inhibitor 100 nM I-RTX on $fA\beta_{1-42}$-induced ROS production (n = 480 untreated; n = 327 I-RTX; n = 344 $fA\beta_{1-42}$; n = 455 $fA\beta_{1-42}$ + I-RTX). B: Inhibitory effects of TRPV1 channel inhibitor 100 nM I-RTX on $sA\beta_{1-42}$-induced ROS production (n = 593 untreated; n = 425 I-RTX; n = 453 $sA\beta_{1-42}$; n = 587 $sA\beta_{1-42}$ + I-RTX). C: Lack of effects of K^+ channel inhibitor 1 μM CTX on $fA\beta_{1-42}$-induced ROS production (n = 480 untreated; n = 404 CTX; n = 344 $fA\beta_{1-42}$; n = 379 $fA\beta_{1-42}$ + CTX). D: Lack of effects of K^+ channel inhibitor 1 μM CTX on $sA\beta_{1-42}$-induced ROS production (n = 593 untreated; n = 342 CTX; n = 453 $sA\beta_{1-42}$; n = 447 $sA\beta_{1-42}$ + CTX). A–D: Fluorescence intensities of DCFDA-loaded cells were normalized to the mean fluorescence intensities determined for untreated control cells. ***$P < 0.001$; n.s., not significant.

ROS production by microglial cells acutely stimulated with either $fA\beta_{1-42}$ or $sA\beta_{1-42}$.

Ion channels regulating microglial priming of NADPH oxidase-mediated ROS production induced by pretreatment with amyloid-β

In a second set of experiments we investigated Aβ-induced priming of NADPH oxidase-mediated ROS production by microglial cells. In these experiments, microglia were kept untreated or were pretreated with either 5 μM fAβ or 5 μM sAβ for 24 h, while microglial ROS production was induced subsequently by stimulation with 1 μM PMA for 1 h in the absence of Aβ. PMA was chosen as secondary stimulus, since PMA directly activates the NADPH oxidase without affecting any other ROS-generating system.

As demonstrated in Fig. 3A, priming of microglia with $fA\beta_{1-42}$ induced significant ($P < 0.001$) upregulation of PMA-stimulated ROS production. Following PMA stimulation, mean DCFDA fluorescence intensities were increased to 342.8 ± 11.3% (n = 610) and to 635.9 ± 17.2 (n = 526) in microglia kept untreated or pretreated with $fA\beta_{1-42}$, respectively. Thus, microglial priming with $fA\beta_{1-42}$ enhanced PMA-induced ROS production to 253.4 ± 6.8% ($P < 0.001$; Fig. 3B). In contrast, pretreatment with the inactive form $fA\beta_{42-1}$ did not cause significant increases ($P = 0.999$) in ROS production when compared with PMA-induced ROS production of microglial cells kept untreated before PMA stimulation (Fig. 3A,B).

Figure 3C demonstrates the priming effects of $sA\beta_{1-42}$ on PMA-induced ROS production by microglial cells. In these experiments, PMA stimulation caused an increase in microglial ROS production to 327.9 ± 13.9% (n = 495; $P < 0.001$) without sAβ pretreatment, whereas PMA-stimulated ROS production was increased to 795.9 ± 51.2% (n = 350; $P < 0.001$) in microglia pretreated with $sA\beta_{1-42}$ for 24 h prior to PMA stimulation. In contrast, the inactive form $sA\beta_{42-1}$ did not induce priming of microglial cells. PMA-stimulated ROS production of microglial cells pretreated with 5 μM $sA\beta_{42-1}$ was almost identical ($P = 0.999$) to that of microglial cells kept untreated before PMA stimulation (Fig. 3C). Figure 3D shows normalized data of the $sA\beta_{1-42}$-induced priming effect on NADPH oxidase-mediated ROS production, while $sA\beta_{1-42}$ was found to cause a significant increase ($P < 0.001$) in PMA-induced ROS production to 283.1 ± 17.1% (n = 350). In comparison, priming effects of PMA-stimulated NADPH oxidase-mediated ROS production induced by either $fA\beta_{1-42}$ or $sA\beta_{1-42}$ were almost identical ($P = 0.072$).

To identify ion channels involved in $A\beta_{1-42}$-induced priming of microglial ROS production, we tested whether simultaneous exposure of microglial cells to ion channel inhibitors and $A\beta_{1-42}$ for 24 h affects subsequent PMA-induced ROS production by microglia. First, microglial cells were pretreated with 100 nM I-RTX and 5 μM $fA\beta_{1-42}$ or 5 μM $sA\beta_{1-42}$. Following washout of $A\beta_{1-42}$ and I-RTX, microglial cells were stimulated with 1 μM PMA for 1 h in the absence of $A\beta_{1-42}$ and I-RTX. As shown in Fig. 4, neither $fA\beta_{1-42}$-induced (Fig. 4A) nor $sA\beta_{1-42}$-induced (Fig. 4B) priming of PMA-induced microglial ROS production was significantly inhibited ($P = 0.094$ for $fA\beta_{1-42}$; $P = 0.725$ for $sA\beta_{1-42}$) by blockade of TRPV1 channels with 100 nM I-RTX.

Furthermore, Fig. 4 summarizes results of the effects of K^+ channel inhibitor CTX on $fA\beta_{1-42}$- and $sA\beta_{1-42}$-induced microglial priming. As shown in Fig. 4C, $fA\beta_{1-42}$-induced priming was unaffected ($P = 0.999$) by inhibition of K^+ channels with 1 μM CTX, whereas $sA\beta_{1-42}$-induced priming of PMA-induced ROS production was significantly ($P < 0.001$) inhibited by 1 μM CTX. Mean DCFDA fluorescence intensities were increased to 286.7 ± 8.6 (n = 749) or to 137.1 ± 6.6% (n = 420) in microglial cells primed with $sA\beta_{1-42}$ in the absence or presence of CTX, respectively.

Since CTX inhibits voltage-gated as well as Ca^{2+}-activated K^+ channels in microglia, we further aimed to identify K^+ channel type(s) involved in the regulation of $sA\beta_{1-42}$-induced priming of NADPH oxidase-mediated ROS production in microglia. Therefore, we additionally tested the effects of MTX, which inhibits Kv1.3 voltage-gated K^+ channels, of TRAM-34, which inhibits KCa3.1 Ca^{2+}-activated K^+ channels, and of paxilline, which blocks KCa1.1 Ca^{2+}-activated K^+ channels. All of these voltage- and Ca^{2+}-activated K^+ channels are sensitive to CTX and are expressed by microglial cells (Eder, 1998, 2010). As shown in Fig. 5A, inhibition of Kv1.3 voltage-gated K^+ channels with 100 nM MTX significantly ($P < 0.001$) reduced $sA\beta_{1-42}$-induced priming of PMA-stimulated ROS production. PMA-induced priming of microglial ROS production was enhanced by $sA\beta_{1-42}$ to 286.7 ± 8.6 (n = 749) or to 141.8 ± 6.6% (n = 467) in the absence or presence of MTX. In comparison, the inhibitory effects of CTX (Fig. 4D) and MTX (Fig. 5A) on $sA\beta_{1-42}$-induced priming were almost identical ($P = 0.999$). In contrast, inhibition of KCa3.1 Ca^{2+}-activated K^+ channels with 1 μM TRAM-34 (Fig. 5B) or blockade of KCa1.1 Ca^{2+}-activated K^+ channels with 1 μM paxilline (Fig. 5C) did not significantly ($P = 0.559$ for TRAM-34; $P = 0.999$ for paxilline) affect $sA\beta_{1-42}$-induced priming of PMA-stimulated ROS production. In summary, these data suggest that the activity of voltage-gated Kv1.3 K^+ channels, but not of Ca^{2+}-activated K^+ channels or of TRPV1 non-selective cation channels, is required for $sA\beta_{1-42}$-induced priming of NADPH oxidase-mediated ROS production.

Discussion

In this study, we demonstrate that in microglia NADPH oxidase activity induced by acute stimulation with Aβ, and NADPH oxidase priming induced by pretreatment with Aβ, are differentially regulated by ion channel activity. We provide the first evidence that functional TRPV1 cation channels are required for Aβ-induced NADPH oxidase-mediated ROS production, and that voltage-gated Kv1.3 K^+ channels are involved in Aβ-induced priming of NADPH oxidase activity.

Importance of TRPV1 channels for sAβ- and fAβ-induced microglial ROS production

Here, we demonstrate that TRPV1 channels, but not K^+ channels, regulate microglial ROS production induced by either $fA\beta_{1-42}$ or $sA\beta_{1-42}$, while a previous publication suggests an additional role of Cl^- channels in Aβ-stimulated microglial NADPH oxidase activity (Milton et al., 2008). In contrast, activity of TRPV1 channels, K^+ channels, H^+ channels, and Cl^- channels was found to be required for microglial ROS production induced by PMA, whereas activity of only TRPV1 channels was sufficient to regulate microglial NADPH oxidase activity induced by lysophosphatidylcholine (Thomas et al., 2007; Schilling and Eder, 2010). Thus, although distinct stimuli lead to the involvement of distinct ion channel types in the regulation of microglial ROS production, activity of TRPV1 channels appears to be an obligatory requirement for induction and/or maintenance of NADPH oxidase activity in microglia independent of the initial stimulus causing microglial activation. The precise mechanisms by which TRPV1 channel activity regulates ROS production in Aβ-stimulated microglia remain to be elucidated. Since NADPH oxidase activity leads to strong membrane depolarization and intracellular acidification (Jankowski and Grinstein, 1999; Eder and DeCoursey, 2001), it is possible that TRPV1 channels are involved in both charge compensation and pH regulation during NADPH oxidase-mediated ROS production by microglial cells. At strong membrane depolarization as seen upon NADPH oxidase activity (Jankowski and Grinstein, 1999), TRPV1 channel activity

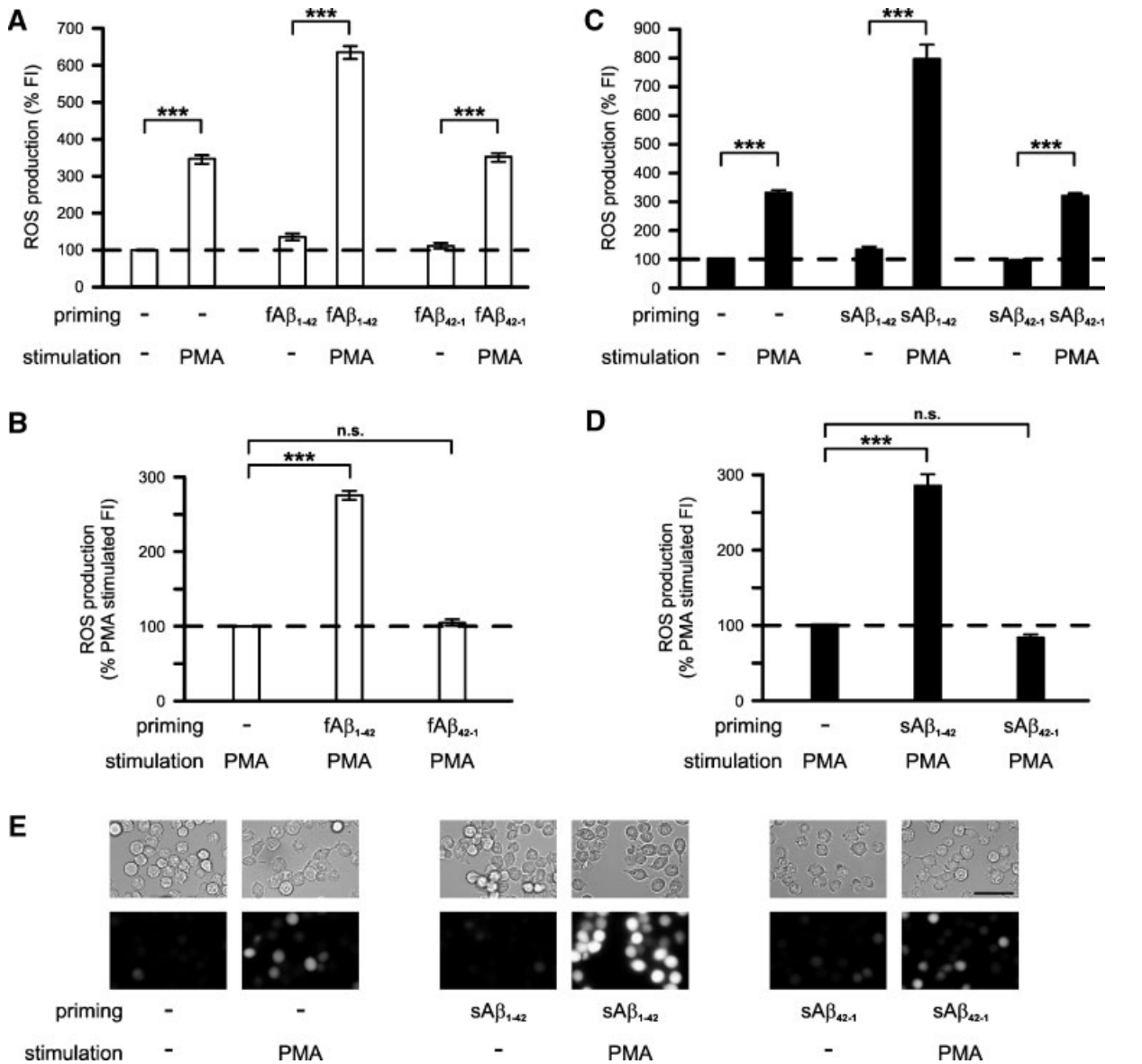

Fig. 3. $A\beta_{1-42}$-induced priming of NADPH oxidase-mediated ROS production by microglial cells. A: Cells were kept untreated or pretreated/primed with either 5 μM $fA\beta_{1-42}$ or 5 μM $fA\beta_{42-1}$ for 24 h, and were subsequently stimulated with 1 μM PMA for 1 h. Bar graphs demonstrate mean fluorescence intensities of DCFDA-loaded cells (n = 651 no priming, no PMA; n = 610 no priming, PMA; n = 306 $fA\beta_{1-42}$ priming, no PMA; n = 526 $fA\beta_{1-42}$ priming, PMA; n = 312 $fA\beta_{42-1}$ priming, no PMA; n = 601 $fA\beta_{42-1}$ priming, PMA). Fluorescence intensities of cells were normalized to the mean fluorescence intensities determined for untreated control cells. B: Priming effects of $fA\beta_{1-42}$ on microglial PMA-induced ROS production. Fluorescence intensities of cells were normalized to the mean fluorescence intensities determined for unprimed PMA-stimulated cells (n = 610 no priming, PMA; n = 526 $fA\beta_{1-42}$ priming, PMA; n = 601 $fA\beta_{42-1}$ priming, PMA). C: Cells were kept untreated or pretreated with either 5 μM $sA\beta_{1-42}$ or 5 μM $sA\beta_{42-1}$ for 24 h, and were subsequently stimulated with 1 μM PMA for 1 h. Bar graphs demonstrate mean fluorescence intensities of DCFDA-loaded cells (n = 606 no priming, no PMA; n = 495 no priming, PMA; n = 533 $sA\beta_{1-42}$ priming, no PMA; n = 350 $sA\beta_{1-42}$ priming, PMA; n = 564 $sA\beta_{42-1}$ priming, no PMA; n = 564 $sA\beta_{42-1}$ priming, PMA). Fluorescence intensities of cells were normalized to the mean fluorescence intensities determined for untreated control cells. D: Priming effects of $sA\beta_{1-42}$ on microglial PMA-induced ROS production. Fluorescence intensities of cells were normalized to the mean fluorescence intensities determined for unprimed PMA-stimulated cells (n = 495 no priming, PMA; n = 350 $sA\beta_{1-42}$ priming, PMA; n = 564 $sA\beta_{42-1}$ priming, PMA). E: Brightfield images (upper row) and fluorescence images (lower row) of DCFDA-loaded microglial cells kept untreated or primed with either 5 μM $sA\beta_{1-42}$ or 5 μM $sA\beta_{42-1}$ for 24 h and subsequently treated without or with 1 μM PMA for 1 h as indicated. Scale bar, 50 μm. $^{***}P < 0.001$; n.s., not significant.

would tend to hyperpolarize cells and would contribute to proton extrusion.

Microglial-generated ROS have neurotoxic effects in a wide variety of neurological diseases, including Alzheimer's disease (e.g., see Block et al., 2007; Block, 2008; Miller et al., 2009). Therefore, better knowledge of the mechanisms underlying microglial ROS production may help to develop therapeutic strategies aiming at the reduction of neurotoxic activities of activated microglia in brain pathology. Microglial NADPH oxidase has already been proposed as potential therapeutic target in Alzheimer's disease and other neuro-degenerative diseases (Sun et al., 2007; Block, 2008; Jaquet et al., 2009). However, general blockade of NADPH oxidase would cause inhibition of ROS generation by all immune cells, including ROS

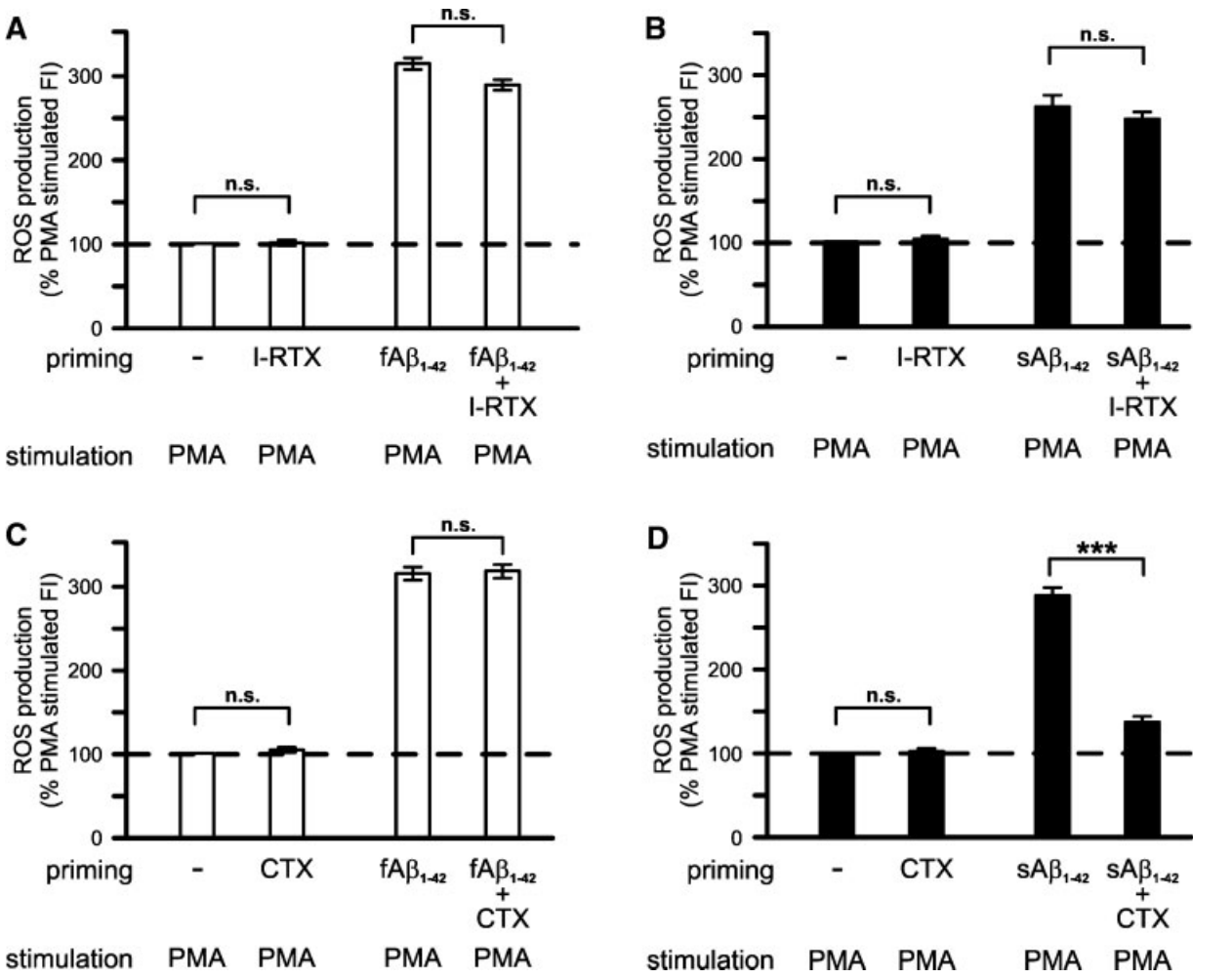

Fig. 4. Importance of ion channels for $fA\beta_{1-42}$- and $sA\beta_{1-42}$-induced priming of NADPH oxidase-mediated ROS production. Prior to stimulation with 1 μM PMA, microglial cells were pretreated with or without $A\beta_{1-42}$ in the presence or absence of ion channel inhibitors as indicated. A: Lack of effects of TRPV1 channel inhibition with 100 nM I-RTX on $fA\beta_{1-42}$-induced priming (n = 508 no priming; n = 425 I-RTX; n = 355 $fA\beta_{1-42}$; n = 384 $fA\beta_{1-42}$ + I-RTX). B: Lack of inhibitory effects of TRPV1 channel inhibitor 100 nM I-RTX on $sA\beta_{1-42}$-induced priming (n = 542 no priming; n = 425 I-RTX; n = 387 $sA\beta_{1-42}$; n = 328 $sA\beta_{1-42}$ + I-RTX). C: Lack of effects of K^+ channel inhibitor 1 μM CTX on $fA\beta_{1-42}$-induced priming (n = 508 no priming; n = 440 CTX; n = 355 $fA\beta_{1-42}$; n = 405 $fA\beta_{1-42}$ + CTX). D: Inhibitory effects of K^+ channel blocker 1 μM CTX on $sA\beta_{1-42}$-induced priming (n = 462 no priming; n = 440 CTX; n = 749 $sA\beta_{1-42}$; n = 420 $sA\beta_{1-42}$ + CTX). A–D: DCFDA fluorescence intensities of cells were normalized to the mean fluorescence intensities determined for unprimed PMA-stimulated cells. ***$P < 0.001$; n.s., not significant.

production by neutrophils, the most important mechanism in bacterial killing, and, thus, would increase the risk of uncontrolled infections. However, since H^+ channels rather than TRPV1 channels mainly regulate ROS production by neutrophils (Murphy and DeCoursey, 2006; De Simoni et al., 2008; DeCoursey, 2010), TRPV1 channels may represent promising targets for specific reduction of microglial ROS-mediated oxidative stress and subsequent neuronal damage without causing general immunosuppression.

Importance of Kv1.3 channels for sAβ-induced priming of microglial NADPH oxidase activity

In healthy brain tissue, microglial cells produce little if any ROS, whereas generation of large quantities of ROS due to enhanced microglial NADPH oxidase activity represents a major mechanism by which activated/primed microglial cells damage surrounding neurons in Alzheimer's disease (Block et al., 2007; Block, 2008). In vitro experiments have revealed that NADPH oxidase-mediated ROS production is enhanced in microglia preincubated, that is, primed, with Aβ (van Muiswink et al., 1996; Klegeris and McGeer, 1997; Colton et al., 2000). In agreement, we were able to induce enhancement of PMA-induced ROS production in microglial cells following pretreatment of cells with Aβ. To date the role of ion channels in regulating microglial priming of NADPH oxidase activity has remained unrecognized. Here we demonstrate for the first time that the activity of ion channels, namely Kv1.3 voltage-gated K^+ channels, is required for $sA\beta_{1-42}$-induced priming of NADPH oxidase activity in microglial cells.

Intriguingly, inhibition of Kv1.3 voltage-gated K^+ channels with either CTX or MTX inhibited $sA\beta_{1-42}$-induced priming, whereas $fA\beta_{1-42}$-induced priming remained unaffected. These data suggest that priming induced by either $sA\beta_{1-42}$ or $fA\beta_{1-42}$ are regulated via distinct physiological mechanisms. This hypothesis is further supported by our finding that ROS production can still be induced by acute stimulation with $sA\beta_{1-42}$ in microglial cells primed with $fA\beta_{1-42}$ (Schilling and Eder, unpublished data). The molecular mechanisms underlying the process of priming that lead to enhanced NADPH oxidase

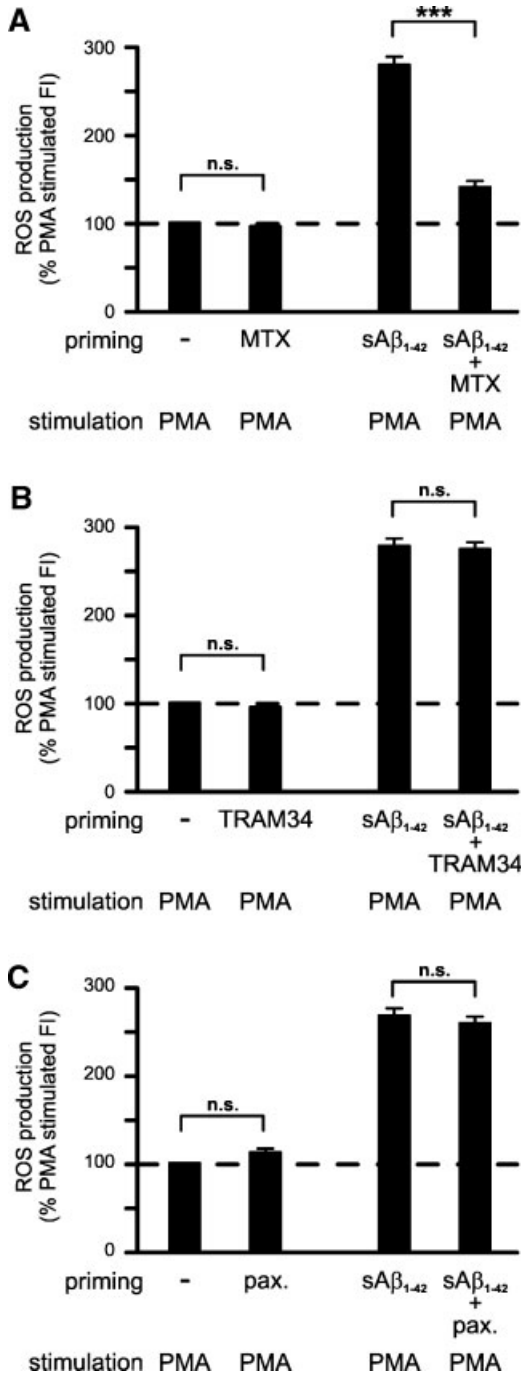

Fig. 5. Effects of K^+ channel inhibitors on $sA\beta_{1-42}$-induced priming. Prior to stimulation with 1 μM PMA, microglial cells were pretreated with or without $sA\beta_{1-42}$ in the presence or absence of K^+ channel inhibitors as indicated. A: Inhibitory effects of Kv1.3 voltage-gated K^+ channel inhibitor 100 nM MTX on $sA\beta_{1-42}$-induced priming (n = 462 no priming; n = 437 MTX; n = 749 $sA\beta_{1-42}$; n = 467 $sA\beta_{1-42}$ + MTX). B: Lack of inhibitory effects of KCa3.1 Ca^{2+}-activated K^+ channel inhibitor 1 μM TRAM-34 on $sA\beta_{1-42}$-induced priming (n = 461 no priming; n = 499 TRAM-34; n = 389 $sA\beta_{1-42}$; n = 418 $sA\beta_{1-42}$ + TRAM-34). C: Lack of inhibitory effects of KCa1.1 Ca^{2+}-activated K^+ channel inhibitor 1 μM paxilline (pax.) on $sA\beta_{1-42}$-induced priming (n = 460 no priming; n = 369 paxilline; n = 371 $sA\beta_{1-42}$; n = 349 $sA\beta_{1-42}$ + paxilline). A–C: Fluorescence intensities of cells were normalized to the mean fluorescence intensities determined for unprimed PMA-stimulated cells. ***$P < 0.001$; n.s., not significant.

activity have so far remained elusive, while increased gene and protein expression of NADPH oxidase components, increased affinity of the oxidase for NADPH, increased cellular protein kinase C (PKC) contents, activation and translocation of PKC to the plasma membrane and other mechanisms have been proposed as possible explanations (reviewed in Sheppard et al., 2005; El-Benna et al., 2008). Thus, due to the lack of precise knowledge of the signaling pathways involved in microglial priming, we can currently only speculate about possible mechanisms by which Kv1.3 voltage-gated K^+ channels regulate NADPH oxidase priming. Since the activity of voltage-gated K^+ channels leads to membrane hyperpolarization, it can be assumed that a negative membrane potential is essential for initiating or maintaining certain cellular processes. For example, increased intracellular Ca^{2+} concentration might be important for optimal activation and translocation of PKC leading to NADPH oxidase priming, while Kv1.3 channel-induced membrane hyperpolarization would enhance Ca^{2+} influx through TRP non-selective cation channels.

It is well recognized and a large body of publications demonstrates that microglial activation in vitro and in vivo is accompanied by the upregulation of voltage-gated Kv1.3 K^+ channels (Eder, 1998, 2010). Although numerous studies have addressed potential roles of Kv1.3 channels in activated microglia, the functional role of these K^+ channels in the transformation from resting into primed microglia has remained unrecognized to date. Using an animal model of Alzheimer's disease, Franciosi et al. (2006) have recently demonstrated that the broad spectrum K^+ channel inhibitor 4-aminopyridine suppressed microglial activation in vivo and reduced microglia-induced neuronal death (Franciosi et al., 2006). These inhibitory effects of 4-aminopyridine, which also blocks Kv1.3 channels in microglia, could be attributed to the inhibition of microglial priming and subsequent reduction of microglial ROS production. Thus, in order to reduce oxidative stress and subsequent neuronal death due to enhanced NADPH oxidase-mediated ROS production by microglia, inhibition of microglial priming by Kv1.3 K^+ channel blockers might also be considered as potential therapeutic strategy in Alzheimer's disease.

In our study, we have focused exclusively on the role of microglial ion channels, which have been found in isolated cultured microglia as well as in microglia in brain tissue, and which can selectively be blocked by highly specific inhibitors. We cannot rule out the possibility that other ion channel types are additionally involved in Aβ-induced ROS production and/or NADPH oxidase priming. In addition, although expression of TRPV1 channels and Kv1.3 channels has been described in microglia of various brain tissue preparations, additional in situ and in vivo experiments are required to verify the importance of these ion channel types in regulating priming and/or activity of microglial NADPH oxidase under physiological and pathophysiological conditions in the brain.

Literature Cited

Bianca VD, Dusi S, Bianchini E, Dal Prà I, Rossi F. 1999. β-Amyloid activates the O_2^- forming NADPH oxidase in microglia, monocytes, and neutrophils. A possible inflammatory mechanism of neuronal damage in Alzheimer's disease. J Biol Chem 274:15493–154939.

Blasi E, Barluzzi R, Bocchini V, Mazzolla R, Bistoni F. 1990. Immortalization of murine microglial cells by a v-raf/v-myc carrying retrovirus. J Neuroimmunol 27:229–237.

Block ML. 2008. NADPH oxidase as a therapeutic target in Alzheimer's disease. BMC Neurosci 9:S8.

Block ML, Zecca L, Hong JS. 2007. Microglia-mediated neurotoxicity: Uncovering the molecular mechanisms. Nat Rev Neurosci 8:57–69.

Colton CA, Chernyshev ON, Gilbert DL, Vitek MP. 2000. Microglial contribution to oxidative stress in Alzheimer's disease. Ann N Y Acad Sci 899:292–307.

De Simoni A, Allen NJ, Attwell D. 2008. Charge compensation for NADPH oxidase activity in microglia in rat brain slices does not involve a proton current. Eur J Neurosci 28:1146–1156.

DeCoursey TE. 2010. Voltage-gated proton channels find their dream job managing the respiratory burst in phagocytes. Physiology 25:27–40.

Eder C. 1998. Ion channels in microglia (brain macrophages). Am J Physiol (Cell Physiol) 275:C327–C342.

Eder C. 2010. Ion channels in monocytes and microglia/brain macrophages: Promising therapeutic targets for neurological diseases. J Neuroimmunol 224:51–55.
Eder C, DeCoursey TE. 2001. Voltage-gated proton channels in microglia. Prog Neurobiol 64:277–305.
El Khoury J, Hickman SE, Thomas CA, Cao L, Silverstein SC, Loike JD. 1996. Scavenger receptor-mediated adhesion of microglia to β-amyloid fibrils. Nature 382:716–719.
El-Benna J, Dang PM, Gougerot-Pocidalo MA. 2008. Priming of the neutrophil NADPH oxidase activation: Role of $p47_{phox}$ phosphorylation and NOX2 mobilization to the plasma membrane. Semin Immunopathol 30:279–289.
Franciosi S, Ryu JK, Choi HB, Radov L, Kim SU, McLarnon JG. 2006. Broad-spectrum effects of 4-aminopyridine to modulate amyloid β_{1-42}-induced cell signaling and functional responses in human microglia. J Neurosci 26:11652–11664.
Jan A, Hartley DM, Lashuel HA. 2010. Preparation and characterization of toxic Aβ aggregates for structural and functional studies in Alzheimer's disease research. Nat Protoc 5:1186–1209.
Jankowski A, Grinstein S. 1999. A noninvasive fluorimetric procedure for measurement of membrane potential. Quantification of the NADPH oxidase-induced depolarization in activated neutrophils. J Biol Chem 274:26098–26104.
Jaquet V, Scapozza L, Clark RA, Krause KH, Lambeth JD. 2009. Small-molecule NOX inhibitors: ROS-generating NADPH oxidases as therapeutic targets. Antioxid Redox Signal 11:2535–2552.
Judge SI, Lee JM, Bever CT Jr, Hoffman PM. 2006. Voltage-gated potassium channels in multiple sclerosis: Overview and new implications for treatment of central nervous system inflammation and degeneration. J Rehabil Res Dev 43:111–122.
Klegeris A, McGeer PL. 1997. β-Amyloid protein enhances macrophage production of oxygen free radicals and glutamate. J Neurosci Res 49:229–235.
Mandrekar-Colucci S, Landreth GE. 2010. Microglia and inflammation in Alzheimer's disease. CNS Neurol Disord Drug Targets 9:156–167.
McDonald DR, Brunden KR, Landreth GE. 1997. Amyloid fibrils activate tyrosine kinase-dependent signaling and superoxide production in microglia. J Neurosci 17:2284–2294.
Miller RL, James-Kracke M, Sun GY, Sun AY. 2009. Oxidative and inflammatory pathways in Parkinson's disease. Neurochem Res 34:55–65.
Milton RH, Abeti R, Averaimo S, DeBiasi S, Vitellaro L, Jiang L, Curmi PM, Breit SN, Duchen MR, Mazzanti M. 2008. CLIC1 function is required for β-amyloid-induced generation of reactive oxygen species by microglia. J Neurosci 28:11488–11499.
Murphy R, DeCoursey TE. 2006. Charge compensation during the phagocyte respiratory burst. Biochim Biophys Acta 1757:996–1011.
Querfurth HW, LaFerla FM. 2010. Alzheimer's disease. N Engl J Med 362:329–344.
Rangaraju S, Chi V, Pennington MW, Chandy KG. 2009. Kv1.3 potassium channels as a therapeutic target in multiple sclerosis. Expert Opin Ther Targets 13:909–924.
Rodrigue KM, Kennedy KM, Park DC. 2009. β-Amyloid deposition and the aging brain. Neuropsychol Rev 19:436–450.
Schilling T, Eder C. 2009. Importance of the non-selective cation channel TRPV1 for microglial reactive oxygen species generation. J Neuroimmunol 216:118–121.
Schilling T, Eder C. 2010. Stimulus-dependent requirement of ion channels for microglial NADPH oxidase-mediated production of reactive oxygen species. J Neuroimmunol 225:190–194.
Schlachetzki JC, Hüll M. 2009. Microglial activation in Alzheimer's disease. Curr Alzheimer Res 6:554–563.
Sheppard FR, Kelher MR, Moore EE, McLaughlin NJ, Banerjee A, Silliman CC. 2005. Structural organization of the neutrophil NADPH oxidase: Phosphorylation and translocation during priming and activation. J Leukoc Biol 78:1025–1042.
Stock C, Schilling T, Schwab A, Eder C. 2006. Lysophosphatidylcholine stimulates IL-1β release from microglia via a $P2X_7$ receptor-independent mechanism. J Immunol 177:8560–8568.
Sun GY, Horrocks LA, Farooqui AA. 2007. The roles of NADPH oxidase and phospholipases A_2 in oxidative and inflammatory responses in neurodegenerative diseases. J Neurochem 103:1–16.
Thomas MP, Chartrand K, Reynolds A, Vitvitsky V, Banerjee R, Gendelman HE. 2007. Ion channel blockade attenuates aggregated alpha synuclein induction of microglial reactive oxygen species: Relevance for the pathogenesis of Parkinson's disease. J Neurochem 100:503–519.
van Muiswinkel FL, Veerhuis R, Eikelenboom P. 1996. Amyloid β protein primes cultured rat microglial cells for an enhanced phorbol 12-myristate 13-acetate-induced respiratory burst activity. J Neurochem 66:2468–2476.